



Oxidative desulfurization of a model fuel using MoO₃ nanoparticles supported on carbon nanotubes catalyst: Examine most significance variables, optimization, kinetics and thermodynamics study

Hameed Hussein Alwan*

Chemical Engineering Department /University of Babylon, Babylon, Hilla, Iraq

ARTICLE INFO

Keywords:

Oxidative desulfurization
Plackett-burman design
Box-behnken experimental design
ANOVA
Reaction kinetics

ABSTRACT

Molybdenum oxide nanoparticles MONP were dispersed on multiwall nanotubes MWNTs as an attempt to synthesize MONP/MWNTs catalyst, the synthesis method done by wet impregnation. The prepared catalyst was characterized by FTIR (Fourier Transform Infrared Spectroscopy) and, XRD (X-ray diffraction), whilst the catalyst activity is done with catalytic oxidative desulfurization ODS reaction for oxidation dibenzothiophene DBT dissolved in heptane (model fuel) with hydrogen peroxide H₂O₂, in which catalyst activity investigation achieved via studying impact six from most affected variables on ODS reaction. The chosen variables are reaction temperature, contact time, sulfur initial sulfur concentration, stirring speed, oxidant/sulfur ratio and catalyst dosage, and then the studied variables were screened by application of Plackett-Burman design PBD to identify the more significant on response (DBT pollutant removal). DBT pollutant removal is referred to as sulfur removal efficiency. Analysis of variance ANOVA shows that the reaction temperature, oxidant/sulfur ratio, stirring speed, and sulfur initial concentration are the most significant from the chosen variables due to their F-values 37.60, 25.45, 11.62 and 6.71 respectively. Box–Behnken experimental design was used to complete the study the effect of the most significant more deeply on ODS reaction (sulfur removal efficiency), in which this part exhibited that sulfur removal efficiency at range between 51 and 93%, whilst the optimum sulfur removal efficiency was 96% at 70 °C, 4.36, 957 rpm and 50 ppm for reaction temperature, oxidant/sulfur ration, stirring speed and initial sulfur concentration respectively. The study involves estimation of kinetics and thermodynamics parameters for ODS reaction; kinetics studying exhibited that ODS reaction followed pseudo-first-order reaction with activation energy (12.996 kJ/mol), while the thermodynamics study shows the low negative entropy change (-0.221 kJ/mol.K), positive enthalpy and free energy changes which confirm a high hydrate transition complex was formed.

1. Introduction

The crude oil as well as its products was contained sulfur, which mainly consists of sulfides, disulfides, thiols and thiophene. These compounds are a source for sulfur oxides SO_x emission after fuel combustion which is not only toxic to human health and pollute environment e.g. acid rain, but also caused corrosion of metal parts in upstream refinery equipment and internal combustion engines (Cedeño-Caero et al., 2008) and (Alwan et al., 2021). The global efforts in the entire world are considered to produce an environmentally friendly fuel from refineries by removing organic sulfur compounds i.e. thiophene and its derivatives as an environmental pollutant (Kayedi et al., 2021).

Dibenzothiophene DBT is characterized as most difficult to remove from fuels in case of using the classical desulfurization technique, and this difficulty appears clearly in the use of hydrodesulphurization reaction HDS; one of the more important limitation of HDS reaction for DBT removing because it has alkyl substituents groups 4 and /or 6 location (Sadare et al., 2017). Oxidative desulfurization ODS can be described as the most important hopeful and promising technique for sulfur removal effectively (Zhang et al., 2014), whatever when comparing between HDS and ODS; ODS can be conducted at room temperature and atmospheric pressure, while HDS reaction requires work at elevated temperature and pressure. Thru the ODS process, the sulfur compound was oxidized to produce Sulfone which described by its strongly polarity,

* Corresponding Author.

E-mail address: hameed@uobabylon.edu.iq.

<https://doi.org/10.1016/j.sajce.2022.03.002>

Received 5 January 2022; Received in revised form 8 February 2022; Accepted 15 March 2022

Available online 16 March 2022

1026-9185/© 2022 The Author(s). Published by Elsevier B.V. on behalf of Institution of Chemical Engineers. This is an open access article under the CC BY-NC-ND license (<http://creativecommons.org/licenses/by-nc-nd/4.0/>).

whereas removed from fuel easily during the extraction step (Bakar et al., 2012). Typically, ODS is conducted by two consecutive steps; oxidation and extraction, the oxidation step achieved in the existence of a catalyst. Many workers and researchers investigated sulfur removal with applying various transition metal oxides such as copper, titanium, manganese, cobalt, tungsten, iron and vanadium as a catalyst for ODS reaction. However, to our knowledge, although there have been some studies on using MoO₃ clusters in Nano scale, but no reports about its startling activity for ODS reaction. Some studies show that MoO₃/SiO₂ can catalyze DBT oxidation by cumene hydroperoxide and other studies stated that MoO₃ supported on alumina Al₂O₃ shows high activity than those on titanium dioxide and silica –alumina (Afsharpour and Dini, 2019).

Many variables assigned are effect on ODS reaction such as sulfur initial concentration, contact time, reaction temperature, stirring (agitation) speed, catalyst dosage, oxidant to sulfur ratio, extraction solvent to volumetric ration, etc. (Alwan, 2021). So these factors need for screening to identify the most effected variables on response, thus “screening design” was necessary. The screening design help for quality control process improvement by determining lower and upper limits for a certain factor. Palckett-Burman experimental design PBD is most common type of screening method and it can be used to study the effects of studied variables on response. The orthogonal matrices devised by Plackett and Burman are useful in examination which leads to fair estimates if all major effects in the smallest possible design (Karlupudi et al., 2018).

In the following study, the MONP/MWNTs catalyst was synthesized by wet impregnation multi-walled carbon nanotubes with molybdenum oxide nanoparticles. The activity of the prepared catalyst was tested for the ODS reaction for removing the DBT pollutant (sulfur source) from the fuel model (heptane). The activity investigation consists of a screening of the most significant operation parameters as well as their role impact on ODS reaction progressing. Activity examination involves of analysis and optimization of removing sulfur results. The ODS reaction kinetics and thermodynamics parameters were estimated in this study.

2. Experimental work

2.1. Materials

Analytical grade chemicals were used; heptane, dibenzothiophene DBT (Riedel-de Haen company), 30 wt.% hydroxide peroxide H₂O₂ (PRS Panerac company), AHM ammonium heptamolybdate (NH₄)₆Mo₇O₂₄•4H₂O (HIPKIN & WILLIAMS company), nitric acid HNO₃ (CHD company), Acetonitrile CH₃CN (Biosolve company) and, Multiwall nanotubes MWNTs (purity >95%, outside diameter 23–30 nm, length 10–30 μm and specific surface are SSA =110 m² / g) purchased from the local market.

2.2. Preparation of synthesis

MoO₃ nanoparticles MONP synthesis by precipitation from aqueous solution AHM, where 5 g from AHM was dissolved in deionized water DW under continues severe mixing and heating at 70 °C to prepare AHM solution. Hot nitric acid was added drop by drop with continued keeping the mixture at 70 °C for 2 h and continued severe mixing, after that the solution was left to cool temperature overnight, the MoO₃ nanoparticles appeared as a precipitate. MONPs were gained by filtration of the solution followed by drying at 110 °C for 6 h.

Preparation of MONP/MWNTs catalyst was done by wet impregnation where 10 g from MWNTs poured into three-neck round flask that immersed in water bath and connected to a vacuum pump to evacuated the humidity may be founded with MWNTs, water bath was adjusted at 50 °C while the vacuum pump was switched on. MONP (1.857 g) were dissolved in DW at 60 °C for MONP/MWNTs catalyst production contain

Table 1

The selected studied variables with their levels.

	Factor	Low level	High level
1	Reaction Temperature (°C) A	40	60
2	Contact Time (minutes) B	10	60
3	Initial sulfur concentration (ppm) C	100	400
4	Stirring speed (rpm) D	200	1000
5	oxidant/sulfur ratio (-) E	1:10	1:1
6	Catalyst dosage (g) F	0.1	0.3

15 wt.% molybdenum .MONP solution was transferred into a separation funnel and dropped inside a three-neck bottom flask that contained evacuated and dried MWNTs. The MONP/MWNTs catalyst was heated to evaporate water followed by drying at 110 °C for 4 h, finally MONP/MWNTs were calcinated at 400 °C for 2 h. The MONP/MWNTs catalyst was characterized using Fourier - Transform Infrared Spectroscopy FTIR spectra (BRUKER Model PLATINUM-ATR Alpha series Germany) over the range 4000–400 cm⁻¹ at room temperature. X-ray diffraction XRD pattern (Shimadzu Model XRD - 6000 Japan).

2.3. Oxidative desulfurization procedure

The ODS reaction was done under the effect of the following independent variables; reaction temperature, reaction time, initial sulfur concentration, stirring speed, oxidant/sulfur ratio and catalyst dosage which symbolic A, B, C, D, E and, F respectively in PBD matrix (Table 2). 100 ml of model fuel (DBT dissolved in heptane) is heated till reached to the specified temperature, after that the specific volume of H₂O₂ with the dosage of catalyst; the mixture was mixed at the defining stirring speed in the reactor (the reactor is 250 ml beaker), the reaction was stopped at the specified time (all parameters were adjusted according to their values listed in Table 2). After reaction completion, an aqueous and oil phases were separated, and then a sample of oil was decanted to second step (extraction with acetonitrile). The total sulfur content (final sulfur concentration) was measured by X-ray fluorescence (Sulfur Meter model RX-620SA/Tanka Scientific) to calculate sulfur removal efficiency via the following equation:

$$R \% = \frac{S_0 - S_f}{S_0} \times 100 \quad (1)$$

Where R% is sulfur removal efficiency, S₀ and S_f are the initial and final total sulfur content respectively.

2.4. Examination of more significant variables by PBD

Six selected variables assigned as controlled variables for ODS reaction were screened by PBD design, PBD can recognize the major variables affecting ODS by doing a limited numbers of experiments (runs) and in another method, it's a screening factors way by aim of analysis of variance ANOVA (Plackett et al., 1946), Table 1 shows the low and high levels for each of chosen factors, where the selected range of the studied variables was assigned according to many pervious work on oxidative desulfurization (Alwan et al., 2020) and, (Alwan, 2021).

3. Experimental design

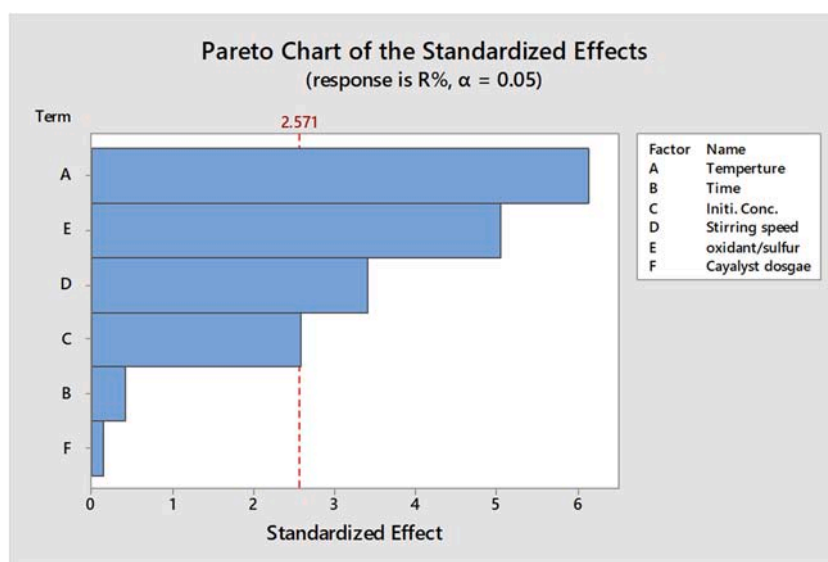
3.1. Screening of most significant factors

The influence of most significant variables upon ODS reaction on MONP/MWNTs catalyst was evaluated by PBD experimental design. Although many numbers of controlled variables on ODS reaction, where some of these variables have a high significance in reaction, while some others have low significance on ODS reaction, or the effect variables may not be the same for each on the ODS reaction. PBD experimental design can be used for screening of impact of studied variables. Factorial design

Table 2

The results of PBD experimental design matrix.

Run	Temperature A	Contact Time B	Initial. Sulfur Conc. C	Stirring speedD	oxidant/sulfur ratio E	Catalyst dosage F	R%
1	40	10	400	1000	1/10	0.1	79
2	40	10	100	1000	1/10	0.3	81
3	60	10	100	200	1/10	0.3	83
4	60	10	400	1000	1/1	0.3	91
5	40	10	100	200	1/1	0.1	81
6	40	60	400	1000	1/1	0.3	82
7	60	60	100	1000	1/1	0.1	93
8	60	10	400	200	1/1	0.1	89
9	60	60	100	1000	1/10	0.1	89
10	40	60	400	200	1/10	0.1	72
11	40	60	100	200	1/1	0.3	85
12	60	60	400	200	1/10	0.3	80

**Fig. 1.** Main effect of studied variables on sulfur removal efficiency by ODS reaction shown by Pareto chart of standard effect based on PBD design.**Table 3**

The ANOVA results for evaluation of mathematical models of sensitivity of studied variables on ODS reaction according to PBD.

Source	DF	Adj. SS	F-Value	P-Value
Model	6	365.833	13.60	0.006
Linear	6	365.833	13.60	0.006
Reaction Temperature	1	168.750	37.64	0.002
Contact Time	1	0.750	0.17	0.699
Initial sulfur concentration	1	30.083	6.71	0.049
Stirring speed	1	52.083	11.62	0.019
oxidant/sulfur ratio	1	114.083	25.45	0.004
Catalyst dosage	1	0.083	0.02	0.897

application for present system (six factors) with using Minitab version 17. PBD experimental design shows that 12 runs were required to study the impact of chosen variables which is enough to cover the system, [Table 2](#), shows the PBD matrix with their results R% as response value for two levels to each of the studied variables.

The experiments results were analyzed by PBD with aim of Minitab software, in which the analysis shows that the order of the most significant factors on ODS reaction according to 95% confidence level is reaction temperature, oxidant/sulfur ratio, stirring speed and initial sulfur concentration are most as illustrated in [Fig. 1](#) for Pareto plot which identity by ANOVA analysis according to their F-values 37.60, 25.45, 11.62, and 6.71 for temperature, oxidant/sulfur ratio, stirring speed and initial sulfur concentration respectively as seen in [Table 3](#), while R^2 is 85%, and adj. R^2 is 87.3%; the regression equation in

uencoded units is:

$$R\% = 65.03 + 0.375A - 0.01B - 0.01056C + 0.00521D - 3.083E - 0.83F \quad (2)$$

It was well known that sulfur removal efficiency increased with reaction temperature, implying the performance of ODS was enhanced with increasing reaction temperature and this was probably due to self-decomposition for H_2O_2 as temperature increased which given that it has a direct effect on reaction rate ([Trakarnpruk and Rujiraworawut, 2009](#)), ([Dedual et al., 2014](#)) ([Salmasi et al., 2016](#)) and, ([Fu et al., 2018](#)) . Temperature and oxidant / sulfur ratio play important rule in DBT oxidation ([Alwan et al., 2020](#)) and ([Lorençon et al., 2014](#)), the reaction rate is first increased by increasing oxidant/sulfur ratio until it is stabilized by adding more oxidation but increasing but increasing H_2O_2 (oxidant/sulfur ratio) results in a lower reaction rate. With the increase of H_2O_2 , there is more and more space occupied by the aqueous solution which leads to the decreasing adsorption of sulfur compounds and the agglomeration of the catalyst. The desulfurization was decreased with initial sulfur concentration ([Shen et al., 2016](#)) . The mixing speed was provided an adequate contact between the two-phase system which improves the desulfurization in ODS ([Choi et al., 2016](#)). Further analysis shows that optimum conditions for maximum removal efficiency are 94.5% at operation condition; 60 °C, 10 min, 100 ppm, 1000 r m p, 1/1, and 0.1 g for temperature, reaction time, initial sulfur concentration, stirring speed, oxidant/sulfur ratio, and catalyst dosage respectively.

Table 4
Independent (controllable) variables and their levels.

Variables, unit	Symbol	Levels			
	coded	Actual	-1	0	1
Reaction Temperature, °C.	x_1	X_1	50	60	70
oxidant/sulfur ratio (-)	x_2	X_2	1	5.5	10
Stirring speed, rpm.	x_3	X_3	600	900	1200
Initial BDT concentration ppm	x_4	X_4	50	100	150

3.2. Box –Behnken experimental design and optimization

The next step is studying the influence of reaction temperature, oxidant/sulfur ratio, stirring speed, and initial sulfur concentration on sulfur removal efficiency (DBT pollutant removal) more deeply, and this will be done by using Box-Behnken experimental design BBD combining with RSM for more significant variables; thus four variables with three levels. RSM method involves of grouping empirical techniques keen to the assessment of relationships existing between a cluster of controlled (studied) variables and measured responses according to one or more selected criteria (Bayraktar, 2001). Box-Behnken design technique has the capability to study experiments with a minimum number of experiments with a higher degree of accuracy compared with conventional methods. The number of experiments required to cover the factors range

Table 5
The BBD matrix and the experimental results.

Design parameters					Design parameters					Design parameters				
Run	x_1	x_2	x_3	x_4	Run	x_1	x_2	x_3	x_4	Run	x_1	x_2	x_3	x_4
1	-1	-1	0	0	10	1	0	0	0	19	-1	0	1	0
2	1	-1	0	0	11	-1	0	0	1	20	1	0	1	0
3	1	1	0	0	12	1	0	0	1	21	0	-1	0	-1
4	-1	1	0	0	13	0	-1	-1	0	22	0	1	0	-1
5	1	0	-1	-1	14	0	1	-1	0	23	0	-1	0	1
6	0	0	1	-1	15	0	-1	1	0	24	0	1	0	1
7	0	0	-1	1	16	0	1	1	0	25*	0	0	0	0
8	0	0	1	1	17	-1	0	-1	0	26*	0	0	0	0
9	-1	0	0	0	18	1	0	-1	0	27*	0	0	0	0

was established according to the Box-Behnken matrix which is calculated by below equation (Ferreira et al., 2007):

$$N = 2k(k - 1) + r \quad (3)$$

Where N is the number of required runs, k is the number of studied factors, and r is the repeated number of central points (3 –6).

Table 4, shows X_1 , X_2 , X_3 and X_4 which refer to reaction temperature, oxidant/sulfur ratio, stirring speed, and initial DBT concentration respectively which selected for this design at three levels low (-1), intermediate (0), and high (+1) values. The coded variables (x_1 , x_2 , and x_3) were related to (un-coded) actual variables by following Eq. (3):

$$x_i = \frac{X_i - X_0}{X_i} \quad i = 1, 2, 3 \quad (4)$$

Where X_0 is central point for the independent (studied) variable (i), and ΔX is the interval value. the matrixes for Box-Behnken was for optimization of the ODS reaction in terms of estimated of the impact of reaction temperature, oxidant/sulfur ratio, stirring speed, and initial DBT concentration on the sulfur removal efficiency, the experimental observation arranged at random orders, Table 5 shows BBD matrix for the all experiments which cover the range of studied variables with their levels.

The RSM is appropriate approximation to find the true relationship between dependent (response) variable with independent (studied)

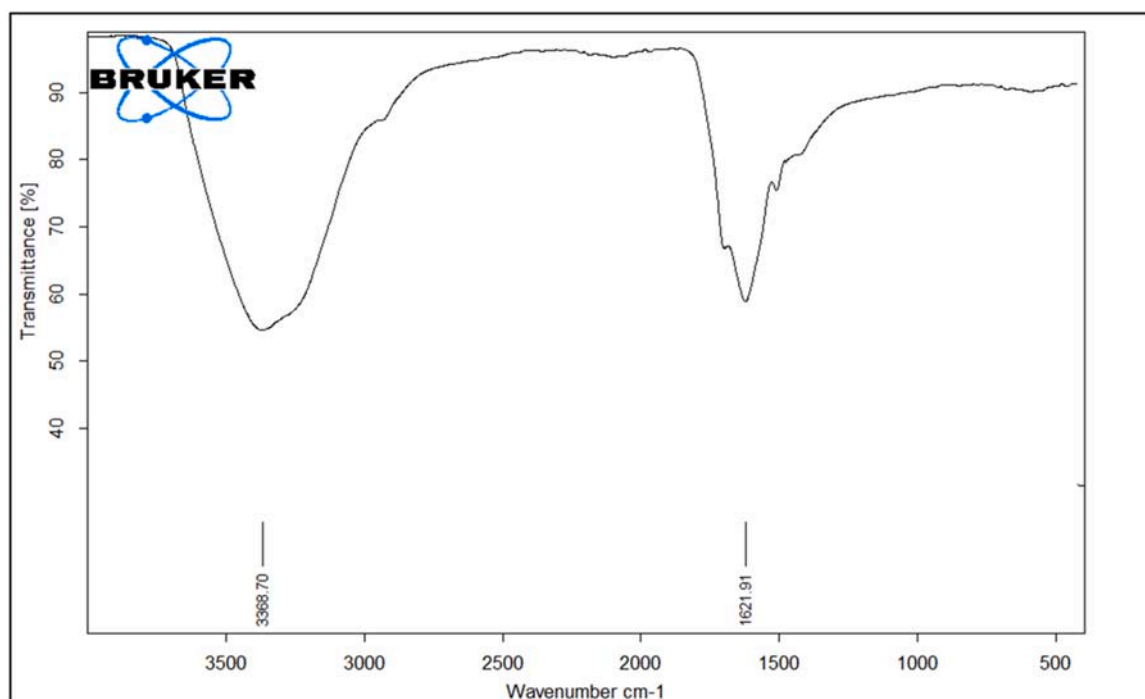


Fig. 2. FTIR spectroscopy for MONP/MWNTs catalyst.

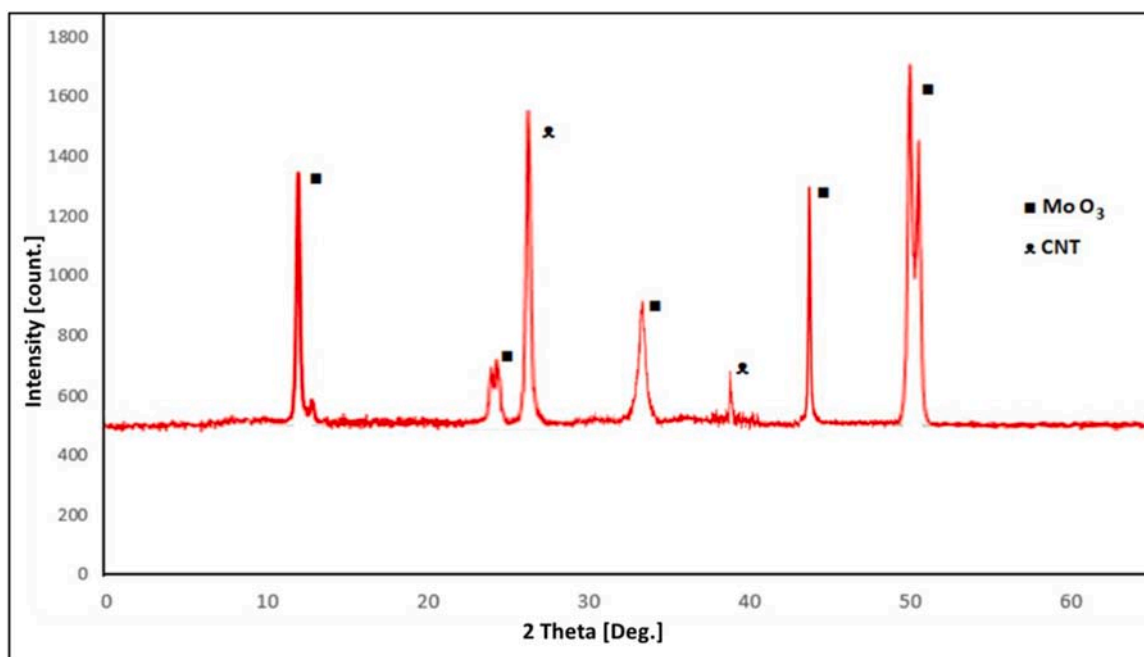


Fig. 3. XRD pattern for MONP/MWNTs catalyst.

Table. 6

The CCD matrix and the experimental results.

Run	Coded variables				Real variables				R%
	x_1	x_2	x_3	x_4	Reaction Temp. (°C)	oxidant/sulfur ratio (-)	stirring speed (rpm)	Initial. Sulfur Conc.(ppm)	
1	-1	-1	0	0	50	1	900	100	78
2	1	-1	0	0	70	1	900	100	87
3	-1	1	0	0	50	10	900	100	68
4	1	1	0	0	70	10	900	100	78
5	0	0	-1	-1	60	5.5	600	50	79
6	0	0	1	-1	60	5.5	1200	50	83
7	0	0	-1	1	60	5.5	600	150	52
8	0	0	1	1	60	5.5	1200	150	83
9	-1	0	0	0	50	5.5	900	50	87
10	1	0	0	0	70	5.5	900	50	93
11	-1	0	0	1	50	5.5	900	150	83
12	1	0	0	1	70	5.5	900	150	81
13	0	-1	-1	0	60	1	600	100	66
14	0	1	-1	0	60	10	600	100	51
15	0	-1	1	0	60	1	1200	100	70
16	0	1	1	0	60	10	1200	100	73
17	-1	0	-1	0	50	5.5	600	100	71
18	1	0	-1	0	70	5.5	600	100	65
19	-1	0	1	0	50	5.5	1200	100	89
20	1	0	1	0	70	5.5	1200	100	92
21	0	-1	0	-1	60	1	900	50	78
22	0	1	0	-1	60	10	900	50	80
23	0	-1	0	1	60	1	900	150	64
24	0	1	0	1	60	10	900	150	83
25	0	0	0	0	60	5.5	900	100	84
26	0	0	0	0	60	5.5	900	100	83
27	0	0	0	0	60	5.5	900	100	80

variables. If the information about the shape of the real response surface is insufficient, the model (generally a first-order model) is upgraded by adding high-level terms to it, so the behavior of the system is explained by the following quadratic equation (Can et al., 2006) and (Yetilmezsoy et al., 2009).

$$y = \beta_0 + \sum_{i=1}^k \beta_i x_i + \sum_{i=1}^k \beta_{ii} x_i^2 + \sum_{i=j}^k \sum_j \beta_{ij} x_i x_j + \varepsilon \quad (5)$$

Where y is predicted response (dependent variable), i, j are index

number, β_0 is intercept term, β_i is linear coefficient, β_j is squared (quadratic) coefficient, β_{ij} is interaction effect, while stands for the random error.

4. Result and discussion

4.1. Catalyst characterization

As seen in Fig. 2, the FTIR spectroscopy shows vibration spectra for MONP/MWNTs catalyst, the peaks in range 3412 and 2926 cm^{-1} appear

Table 7
Regression Equation in Un-Coded Units.

Source	DF	Adj.SS	Adj.MS	F-Value	P-Value
Model	14	2592.69	185.192	5.52	0.0000003
x ₁	1	34.68	34.680	1.03	0.0000032
x ₂	1	9.40	9.399	0.28	0.0000606
x ₃	1	924.71	924.710	27.57	0.00000000
x ₄	1	245.35	245.346	7.31	0.0019125
x ₁ ²	1	86.19	86.189	7.57	0.0000003
x ₂ ²	1	345.83	345.828	2.57	0.0013522
x ₃ ²	1	361.90	361.901	10.31	0.0000007
x ₄ ²	1	2.43	2.430	10.79	0.0000007
x ₁ × x ₂	1	0.34	0.336	0.07	0.0079212
x ₁ × x ₃	1	18.75	18.749	0.01	0.000922
x ₁ × x ₄	1	14.98	14.977	0.56	0.0004691
x ₂ × x ₃	1	82.63	82.628	2.46	0.0005147
x ₂ × x ₄	1	71.57	71.57	2.13	0.0001702
x ₃ × x ₄	1	175.03	175.033	5.22	0.00004133

to arise by H—O—H and O—H bending of water, the peak at 798 cm⁻¹ related to Mo—O—Mo while the peak at range 505–540 cm⁻¹ associated to Mo—O bond, and peak at 453 cm⁻¹ indicated the broadening vibration oxygen atoms linked to three atoms of molybdenum (Fang et al., 2007) and (Gowtham et al., 2018) Fig. 3., shows the XRD pattern of MONP/MWNTs catalyst. Its shows the XRD for MoO₃ nanoparticles dispersed on carbon nanotubes, the reflections of at 2θ = 12.6, 23.4, 33.5, 45.9 and 49.1° which indicates the presence of MoO₃ that corresponded (020), (110), (130), (111) and (041) to planes (JCPDS 35–0609), while the reflections at 2θ = 27.4 and 39.2 which refers to the presence of MWNTs that corresponded to planes (002) and (100) (JCPDS 41–1487) (Dedual et al., 2014) (Gowtham et al., 2018).

4.2. Estimation model and statistical assessment

The observed results for the impact of reaction temperature, oxidant/sulfur ratio, stirring speed and initial sulfur concentration on ODS reaction were listed in Table 6, seen the results exhibited removal efficiency range between (51%–93%). The actual results were fitted according to second-order polynomial by using Minitab software, and it can be used to predict optimum point, for four variables where the second-order polynomial represents by Eq. (4).

By applying Eq. (5) with response results given in Table 6, the following second order polynomial equation was established which explain the sulfur removal efficiency as a function of studied variables (coded values):

$$y = 82.19 + 1.7x_1 - 0.88x_2 + 8.78x_3 - 4.52x_4 + 4.02x_1^2 - 8.05x_2^2 - 8.24x_3^2 + 0.68x_4^2 + 0.29x_1x_2 + 2.17x_1x_3 - 1.94x_1x_4 + 4.54x_2x_3 + 4.23x_2x_4 + 6.62x_3x_4 \quad (6)$$

Where y is predicted sulfur removal efficiency, x₁, x₂, x₃, x₄ are the coded term for four independent variables reaction temperature, oxidant/sulfur ratio, stirring speed, and initial sulfur concentration respectively. The optimum predicted values for selected investigation variables were found by solving Eq. (5). The analysis of variance ANOVA is essential to test the most significant variables as well as the order of effect for variables. ANOVA analysis was shown in Table 7, as seen in the Fisher's F-test (F model = 5.52) with a low probability value (P model > = 0.0000003) as Liu et al. reported. The value of the coefficient (R² = 0.91%) and the adjusted R² is 0.89%. Based on the results and ANOVA analysis, the highest impact on sulfur removal efficiency is according to the following orders; stirring speed, initial sulfur concentration, reaction temperature and, oxidant/sulfur ratio via their F-Value 27.57, 7.31, 1.03 and, 0.28 respectively (Liu et al., 2004). The sulfur removal efficiency was increased as the reaction temperature increased maybe because increasing temperature leads to accelerating the rate of reaction via increasing internal motion of reactant molecules (Dedual et al., 2014) (Li et al., 2016) and, (Alwan et al., 2020). The removal efficiency enhanced by the increase of H₂O₂ (oxidant/sulfur ratio) because of the abundance of oxidant agents mean a large amount of oxidant which decomposed to water and oxygen and more oxidation reaction (Gnaser et al., 2004), and (Zhu et al., 2014), while the sulfur removal efficiency decreased as initial sulfur concentration because there are more DBT molecules were adsorbed on the catalyst surface which occupied the active sites at the catalyst surface and this leads reduction of the generation of OH radicals at the catalyst surface (Nezamzadeh-Ejhieh and Karimi-Shamsabadi, 2013). Stirring speed has highest effect, and this is because the stirring (mixing) speed condition has great influence on droplet interface, in which catalyst was founded primarily at oil-water interface. Within lower stirring speed, there are few droplet in the emulsion, these drops characterized by smaller size, thus the rate of reaction is low due to less contact surface area. whenever the stirring speed was increasing there are more and more droplets were formed with larger surface area and uniform shape. At this case the catalyst was well dispersed at interfaces which lead to increasing the reaction rate (D Huang et al., 2006.) and, (Lu et al., 2014). The optimization for the system is state that maximum removal efficiency is 96% at operation conditions; reaction temperature (70°C), oxidant/sulfur ratio (4.36), stirring speed (957 rpm), and initial sulfur concentration (50 ppm) .as

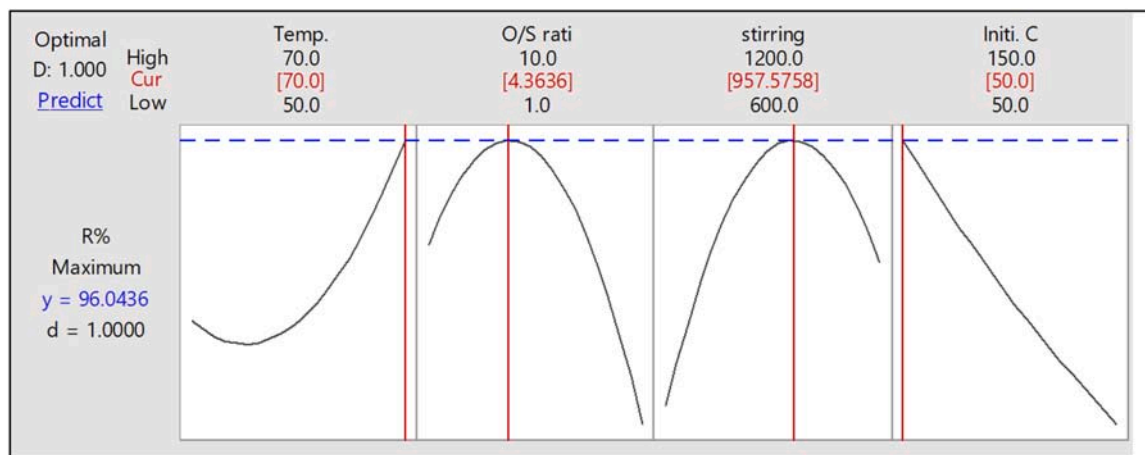


Fig. 4. The maximum sulfur removal efficiency is 96% which can be gotten by applying optimum operations condition at reaction temperature (70 °C), O/S ratio (4.36), stirring rate (957 rpm) and initial sulfur concentration (50 ppm).

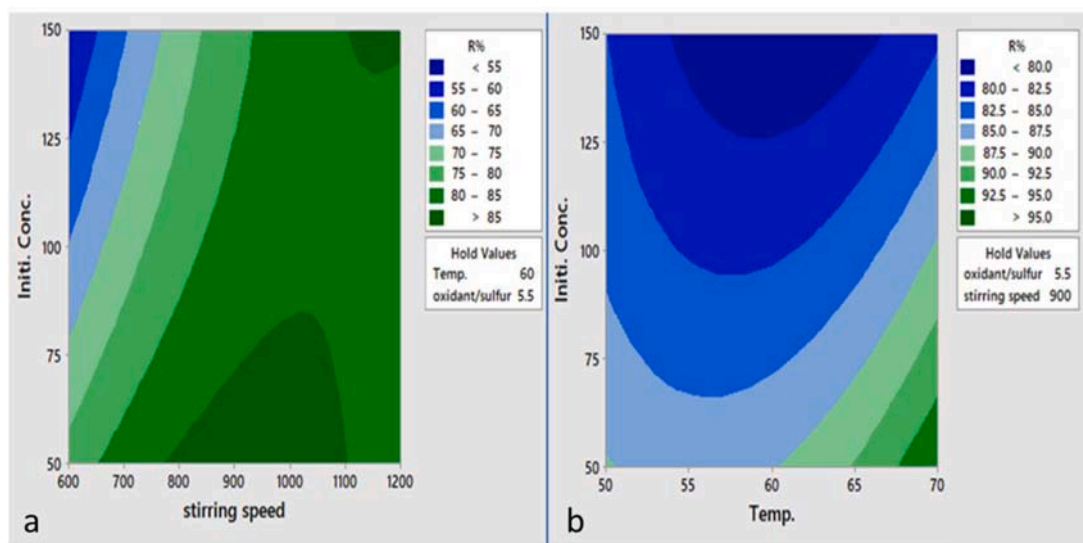


Fig. 5. the interaction effect of (a) initial sulfur concentration and stirring speed on sulfur removal efficiency while holding reaction temperature at 60 °C and oxidant/sulfur ratio at 5.5, (b) initial sulfur concentration and reaction temperature on sulfur removal efficiency while holding oxidant/sulfur ratio at 5.5 and 900 rpm for stirring speed.

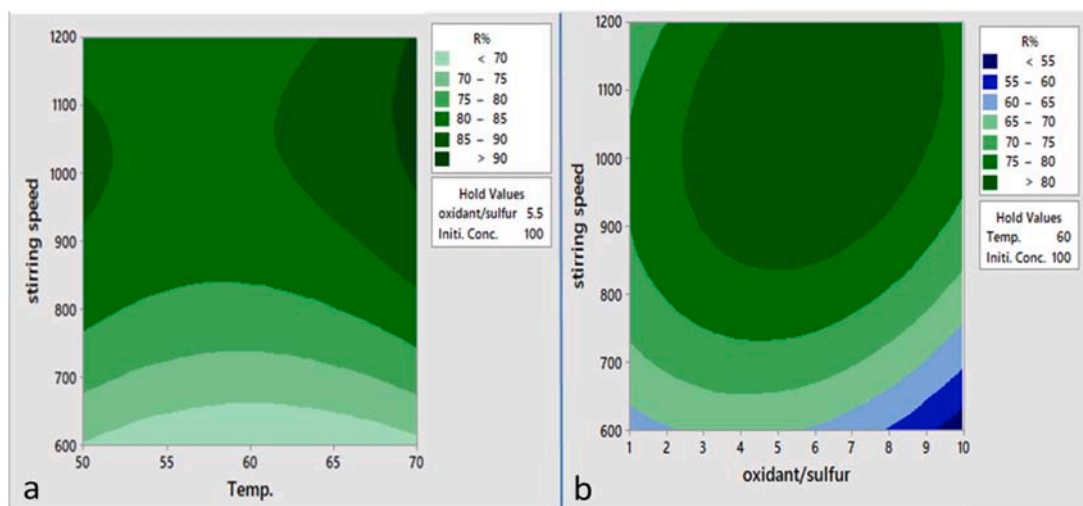


Fig. 6. illustrate contour plots (a) the interactive effects between stirring speed and temperature while other variables were held at their respective center levels; initial DBT concentration 100 ppm and oxidant/sulfur ratio 5.5, (b) the interactive effects between stirring speed and oxidant/sulfur ratio while other variables were held at their respective center levels; temperature at 60°C and initial DBT concentration 100 ppm.

shown in Fig. 4.

4.3. The interaction effect of studied variables

The combined influence of stirring speed and initial sulfur concentration can be seen clearly in Fig. 5-a; for the constant value of initial sulfur concentration (for example 50 ppm) the sulfur removal efficacy increased with mixing speed to value more than 85%, after that it started to decreased (D Huang et al., 2006.), but this behavior is not same when the initial sulfur concentration increasing because the sulfur removal efficiency decreasing with increasing initial sulfur concentration which agree with C. Shen et al. (Shen et al., 2016) . The interaction impact by initial sulfur concentration and temperature is shown in Fig. 5– b at constant temperature the sulfur removal efficiency decreased with increasing initial sulfur because of limited catalyst application range as stated by L. Liantang (Li et al., 2016), but it was increasing with temperature via increasing in reaction rate (Alwan et al., 2020) .

Fig. 6-a showing the interactive effects between reaction

temperature and stirring speed, (b) the interactive effects between initial sulfur concentration and temperature while other variables were held at their respective center levels; stirring speed 900 rpm and oxidant/sulfur ratio 5.5. The combine effect of temperature and stirring speed was shown in Fig. 6-a; mixing speed caused enlarge the droplet so the reaction rate will be high, thus it will be more large with temperature increasing (D Huang et al., 2006.), and (Lu et al., 2014). As seen in Fig. 7, oxidant/sulfur ratio and temperature plays significance roles in DBT oxidation (sulfur removal efficiency), it was noted that the interaction effect of both these variables are complex, but in general at constant oxidant/sulfur ratio, the sulfur removal efficacy increasing with temperature via direct effect of temperature on reaction rate .The effect of temperature can be less noticeable as decreasing of oxidant/sulfur ratio, the temperature impact maybe cause competition reaction between hydrogen peroxide decomposition and DBT oxidation, the reduction in sulfur removal efficiency with oxidant/sulfur ratio is a result of dilution via hydrogen peroxide decomposition (Lu et al., 2014)

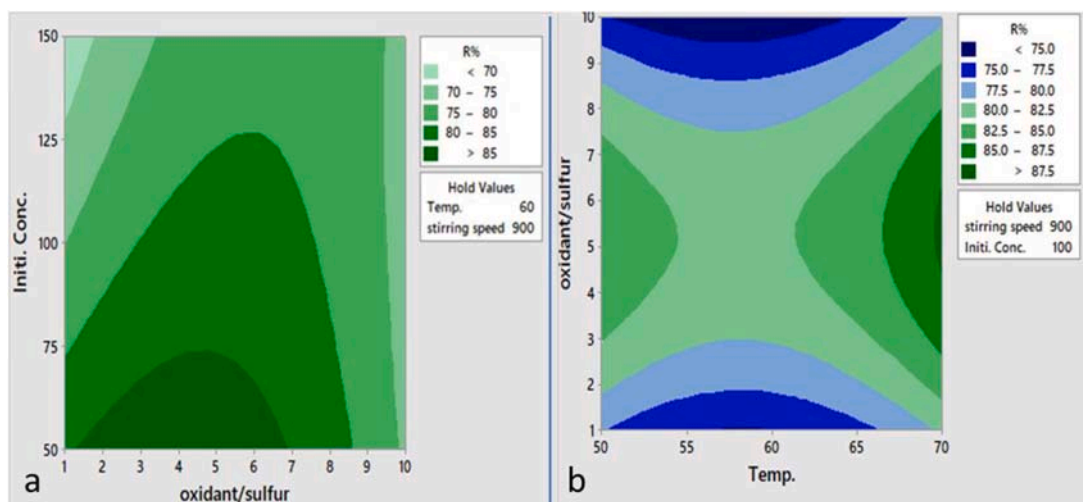


Fig. 7. the interaction effect of (a) initial sulfur concentration against oxidant/sulfur ratio on sulfur removal efficiency while holding stirring speed at 900 rpm and reaction temperature at 60 °C, (b) reaction temperature against oxidant/sulfur ratio on sulfur removal efficiency while holding initial sulfur concentration at 60 °C and reaction temperature at 60 °C.

4.4. Kinetics and thermodynamics of ODS reaction

The study of reaction kinetics done by measured the final sulfur content with time at temperature 50, 60, and 70 °C while kept the other variables at optimum value (900, 4.36 mL and, 0.1 g for stirring speed, oxidant/sulfur ratio and catalyst dosage respectively). Assume the DBT oxidation reaction is:



Therefore the reaction rate equation is as following:

$$-r_A = \frac{-dC_{DBT}}{dt} = kC_{DBT}C_{H_2O_2} \quad (8)$$

Assume that amount of H_2O_2 was represented as excess reactant so the change in H_2O_2 concentration in comparison with DBT can be neglected, so $C_{H_2O_2}$ can be considered as constant. Therefore the reaction may be represented a pseudo first order reaction. The rate is seemingly depended on concentration of limiting reactant C_{DBT} . Thus Eq. (8) can be written as follows:

$$-r_A = \frac{-dC_{DBT}}{dt} = k_{app}C_{DBT} \quad (9)$$

Where $k_{app} = KC_{H_2O_2}$ is apparent reaction rate constant (1/min).

The integration of Eq. (9) with integration limits; $C_{DBT}=C_0$ at time = 0, to $C_{DBT} = C_f$ at time = t.

$$-\ln \frac{C_f}{C_0} = k_{app}t \quad (10)$$

The experimental data was fitted to pseudo first order reaction at different temperatures with too high correlation coefficients confirm (0.9872, 0.9966 and 0.9721) at 50, 60, and 70 °C respectively as shown in Fig. 7. From Eq. (10) the slopes of straight lines represented apparent reaction rate constant; 0.1822, 0.2022 and 0.2418 min^{-1} at 50, 60, and 70 °C respectively. In general the rate constant for first order reaction is related to the reaction temperature as Arrhenius equation stated;

$$k = A \exp \frac{E_a}{RT} \quad (11)$$

Here E_a represented the reaction activation energy, R is universal gas constant, A is pre-exponential factor and T is absolute temperature Eq. (11). can be written as follows:

$$\ln(k) = \ln(A) - \frac{E_a}{RT} \quad (12)$$

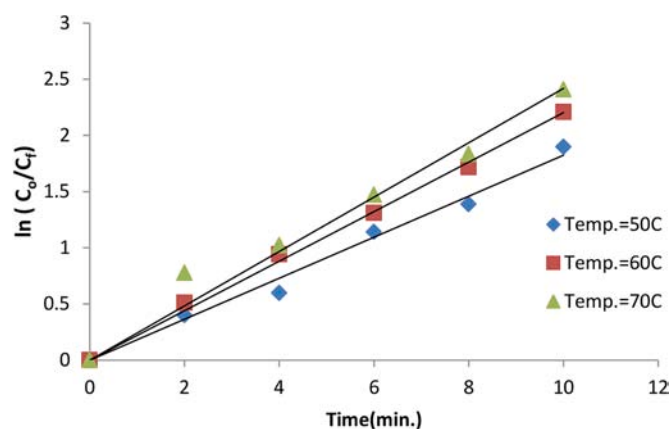


Fig. 8. experimental data fitting to pseudo first order reaction.

Table 8
activation energy for dibenzothiophene for various catalyst / H_2O_2 .

catalyst	activation energy kJ /mol	Reference
$H_3PW_{12}O_{40}$	45.9	(Choi et al., 2016)
$H_3PMo_{12}O_{40}$	29.0	(Choi et al., 2016)
$H_3SiW_{12}O_{40}$	28.3	(Choi et al., 2016)
HPW/aEVM	30.3	(P Huang et al., 2017.)
Fe_2O_3 /Graphene	36.26	(Alwan et al., 2020)

The fitting of reaction rate constant data can be illustrated in Fig. 8, by plotting logarithm k against (1/T), the reaction activation energy was calculated from the slope of straight line ($R^2=0.9719$), thus the value of activation energy is 12.996 kJ/mol. The estimated activation energy for catalytic oxidative desulfurization here is low when compare with some other previous works (listed in Table 8) maybe refers that the MONP/MWNTs catalyst which used here is more active than these other works

Thermodynamics parameters for DBT oxidative desulfurization reaction was estimated as followed; the enthalpy change (ΔH) was calculated from activation energy

$$H = E_a + RT \quad (13)$$

Activation entropy change can be calculated fitting the data with following equation:

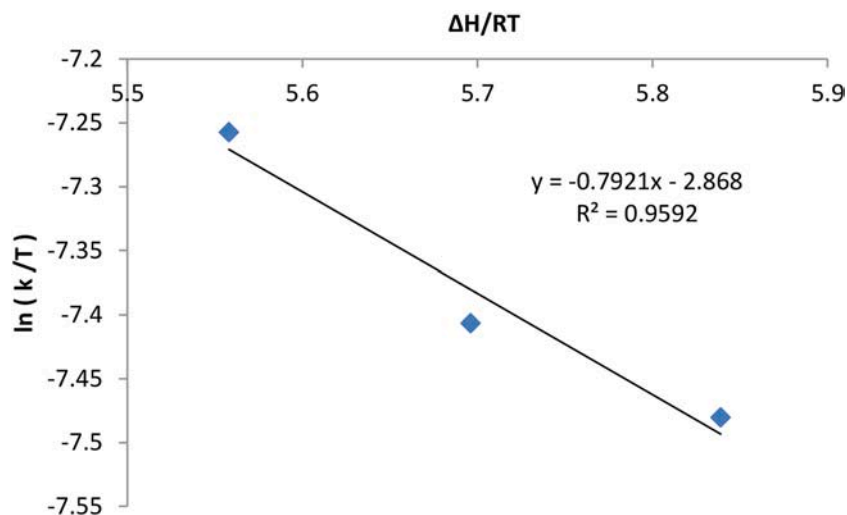


Fig.9. Typical plot used for the estimation of activation entropy for the reaction.

Table 9

Kinetics and thermodynamic parameters for the DBT oxidation.

T (K)	k (sec ⁻¹)	Ea(kJ/ mol)	ΔH(kJ/ mol)	ΔS(kJ/ mol)	ΔG(kJ/ mol)
313	0.1822	12.225	15.68	-0.221	87.02
323	0.2022		15.77		89.36
333	0.2418		15.85		91.65

$$\ln \frac{k'}{T} = \ln \left(\frac{K_B}{h} \right) + \left(\frac{\Delta S}{R} \right) - \left(\frac{\Delta H}{RT} \right) \quad (14)$$

Where K_B is Boltzmann constant ($1.38 \times 10^{-23} \text{ m}^2 \text{ kg s}^{-2} \text{ K}^{-1}$) and, h is Plank constant ($6.626 \times 10^{-34} \text{ m}^2 \text{ kg / s}$) respectively. Therefore plotting of $\ln(k/T)$ against $(\Delta H/RT)$ may give straight line; the line intercept helps to calculate change of entropy. Finally the reaction Gibbs free energy (ΔG) value was estimated by

$$G = H - TS \quad (15)$$

The data obtained from the above were listed on Table 8, as seen, the DBT oxidation reaction.

5. Conclusion

An effective ODS reaction by using MONP/MWNTs catalyst in presence of H_2O_2 as an oxidant agent for model fuel (DBT dissolved in heptane) was investigated at different operation conditions for some selected variables, these variables were screened with Plackett – Burman design method; among the selected variables (reaction temperature, initial sulfur concentration, stirring speed, oxidant/sulfur ratio, catalyst dosage and contact time), it was found that reaction temperature, oxidant/sulfur ratio, stirring speed, and initial sulfur concentration are more significant variables affecting on sulfur removal efficiency. These variables are studied more deeply with Box-Behnken experimental design; the result shows that sulfur removal efficiency was ranged between 51 – 93% while the maximum value is 96% at optimum operation conditions (70 °C, 4.36 ml, 957 rpm and 50 ppm for reaction temperature, oxidant/sulfur ratio, stirring speed and initial concentration respectively) which refers that the synthesized catalyst (MONP/MWNTs) has good activity. The ODS was found to obey pseudo-first-order reaction with activation energy equal 12.966 kJ / mol and reaction rate constants are 0.1822, 0.2022, and 0.2418 min⁻¹ at 50, 60, and 70 °C respectively. The thermodynamics study exhibited the low negative entropy change - 0.221 kJ / mol.K (near zero and it's relatively positive) and positive enthalpy and free energy changes which coliform

a high hydrate transition complex was formed. Eq. (1), 2, 6, 7, 12-15, Fig. 9, Table 9

Declaration of Competing Interest

The authors declare that they have no known competing financial interests or personal relationships that could have appeared to influence the work reported in this paper.

Acknowledgement

The author would like to acknowledge to Department of chemical engineering at university of Babylon for support the work, Mr. Riyadh Noman manager of chemical and petrochemical research center / Corporation of research and industry development / ministry of Industry and minerals and Mr. Quraish, Mr. Zuhair for their help in measuring sulfur content . Dr. Muhammed for doing XRD, and all who help to finish this work.

References

- Afsharpour, M., Dini, Z., 2019. One-pot functionalization of carbon nanotubes by WO₃/MoO₃ nanoparticles as oxidative desulfurization catalysts. Fuller. Nanotub. Carbon Nanostructures 27 (3), 198–205. <https://doi.org/10.1080/1536383X.2018.1538132>.
- Alwan, H.H., Makki, Hasan F., Al, T.A., 2021. Preparation, characterization and, activity of CoMo supported on graphene for heavy naphtha hydro-desulfurization reaction. Iran. J. Catal. 11 (2), 101–111. <http://ijc.iaush.ac.ir/article/682773.html>.
- Alwan, H.H., 2021. Photo catalysis desulfurization at copper oxides /titanium oxide nanotubes. Iran. J. Catal. 11 (4), 363–375.
- Alwan, H.H., Ali, A.A., Makki, H.F., 2020. Optimization of oxidative desulfurization reaction with Fe₂O₃ catalyst supported on graphene using box-behnken experimental method. Bull. Chem. React. Eng. Catal. 15 (1), 175–185. <https://doi.org/10.9767/bcrec.15.1.6670.175-185>.
- Bakar, W.A.W.A., Ali, R., Kadir, A.A.A., Mokhtar, W.N.A.W., 2012. Effect of transition metal oxides catalysts on oxidative desulfurization of model diesel. Fuel Process. Technol. 101, 78–84. <https://doi.org/10.1016/j.fuproc.2012.04.004>.
- Bayraktar, E., 2001. Response surface optimization of the separation of DL-tryptophan using an emulsion liquid membrane. Process Biochem. 37 (2), 169–175. [https://doi.org/10.1016/S0032-9592\(01\)00192-3](https://doi.org/10.1016/S0032-9592(01)00192-3).
- Can, M.Y., Kaya, Y., Algur, O.F., 2006. Response surface optimization of the removal of nickel from aqueous solution by cone biomass of Pinus sylvestris. Bioresour. Technol. 97 (14), 1761–1765. <https://doi.org/10.1016/j.biortech.2005.07.017>.
- Cedeño-Caero, L., Gomez-Bernal, H., Fraustro-Cuevas, A., Guerra-Gomez, H.D., Cuevas-García, R., 2008. Oxidative desulfurization of synthetic diesel using supported catalysts. Part III. Support effect on vanadium-based catalysts. Catal. Today 133–135 (1–4), 244–254. <https://doi.org/10.1016/j.cattod.2007.12.017>.
- Choi, A.E.S., Roces, S., Dugos, N., Wan, M.W., 2016. Mixing-assisted oxidative desulfurization of model sulfur compounds using polyoxometalate/H₂O₂ catalytic system. Sustain. Environ. Res. 26 (4), 184–190. <https://doi.org/10.1016/j.serj.2015.11.005>.

- Dedual, G., Macdonald, M.J., Alshareef, A., Wu, Z., Tsang, D.C.W., Yip, A.C.K., 2014. Requirements for effective photocatalytic oxidative desulfurization of a thiophene-containing solution using TiO₂. *J. Environ. Chem. Eng.* 2 (4), 1947–1955. <https://doi.org/10.1016/j.jece.2014.08.012>.
- Fang, L., Shu, Y., Wang, A., Zhang, T., 2007. Green synthesis and characterization of anisotropic uniform single-crystal α -MoO₃ nanostructures. *J. Phys. Chem. C* 111 (6), 2401–2408. <https://doi.org/10.1021/jp065791r>.
- Ferreira, S.L.C., Bruns, R.E., Ferreira, H.S., Matos, G.D., David, J.M., Brandão, G.C., da Silva, E.G.P., Portugal, L.A., dos Reis, P.S., Souza, A.S., dos Santos, W.N.L., 2007. Box-Behnken design: an alternative for the optimization of analytical methods. *Anal. Chim. Acta* 597 (2), 179–186. <https://doi.org/10.1016/j.aca.2007.07.011>.
- Fu, J., Guo, Y., Ma, W., Fu, C., Li, L., Wang, H., Zhang, H., 2018. Syntheses and ultra-deep desulfurization performance of sandwich-type polyoxometalate-based TiO₂ nanofibres. *J. Mater. Sci.* 53 (22), 15418–15429. <https://doi.org/10.1007/s10853-018-2736-z>.
- Gnaser, H., Huber, B., Ziegler, C., 2004. Nanocrystalline TiO₂ for Photocatalysis 6.
- Gowtham, B., Ponnuswamy, V., Pradeesh, G., Chandrasekaran, J., Aradhana, D., 2018. MoO₃ overview: hexagonal plate-like MoO₃ nanoparticles prepared by precipitation method. *J. Mater. Sci. Mater. Electron.* 29 (8), 6835–6843. <https://doi.org/10.1007/s10854-018-8670-7>.
- Huang, D., Wang, Y.J., Yang, L.M., Luo, G.S., 2006. Chemical oxidation of dibenzothiophene with a directly combined amphiphilic catalyst for deep desulfurization. *Ind. Eng. Chem. Res.* 45 (6), 1880–1885. <https://doi.org/10.1021/ie0513346>.
- Huang, P., Luo, G., Kang, L., Zhu, M., Dai, B., 2017. Preparation, characterization and catalytic performance of HPW/aEVM catalyst on oxidative desulfurization. *RSC Adv.* 7 (8), 4681–4687. <https://doi.org/10.1039/C6RA26587A>.
- Karlapudi, A.P., Krupanidhi, S., E, R.R., M, I., Md, N.B., T.C, V, 2018. Plackett-Burman design for screening of process components and their effects on production of lactase by newly isolated *Bacillus* sp. VUVD101 strain from Dairy effluent. *Beni-Suef Univ. J. Basic Appl. Sci.* 7 (4), 543–546. <https://doi.org/10.1016/j.bjbas.2018.06.006>.
- Kayedi, N., Samimi, A., Asgari Bajgirani, M., Bozorgian, A., 2021. Enhanced oxidative desulfurization of model fuel: a comprehensive experimental study. *S. Afr. J. Chem. Eng.* 35 (August), 153–158. <https://doi.org/10.1016/j.sajce.2020.09.001>.
- Li, L., Zhang, J., Shen, C., Wang, Y., Luo, G., 2016. Oxidative desulfurization of model fuels with pure nano-TiO₂ as catalyst directly without UV irradiation. *Fuel* 167, 9–16. <https://doi.org/10.1016/j.fuel.2015.11.047>.
- Liu, H.L., Lan, Y.W., Cheng, Y.C., 2004. Optimal production of sulphuric acid by *Thiobacillus thiooxidans* using response surface methodology. *Process Biochem.* 39 (12), 1953–1961. <https://doi.org/10.1016/j.procbio.2003.09.018>.
- Lorençon, E., Alves, D.C.B., Krambrock, K., Ávila, E.S., Resende, R.R., Ferlauto, A.S., Lago, R.M., 2014. Oxidative desulfurization of dibenzothiophene over titanate nanotubes. *Fuel* 132, 53–61. <https://doi.org/10.1016/j.fuel.2014.04.020>.
- Lu, M.C., Biel, L.C.C., Wan, M.W., De Leon, R., Arco, S., 2014. The oxidative desulfurization of fuels with a transition metal catalyst: a comparative assessment of different mixing techniques. *Int. J. Green Energy* 11 (8), 833–848. <https://doi.org/10.1080/15435075.2013.830260>.
- Nezamzadeh-Ejehieh, A., Karimi-Shamsabadi, M., 2013. Decolorization of a binary azo dyes mixture using CuO incorporated nanozeolite-X as a heterogeneous catalyst and solar irradiation. *Chem. Eng. J.* 228, 631–641. <https://doi.org/10.1016/j.cej.2013.05.035>.
- Plackett, R.L., Burman, J.P., Plackett, R.L., Burman, J.P., 1946. The Design of Optimum Multifactorial Experiments Author (s), 33. Published by : Biometrika Stable, pp. 305–325. URL. <http://www.jstor.org/stable/2333333>.
- Sadare, O.O., Obazu, F., Daramola, M.O., 2017. Biodesulfurization of petroleum distillates—Current status, opportunities and future challenges. *Environments - MDPI* 4 (4), 1–20. <https://doi.org/10.3390/environments4040085>.
- Salmasi, M., Fatemi, S., Mortazavi, Y., 2016. Fabrication of promoted TiO₂ nanotubes with superior catalytic activity against TiO₂ nanoparticles as the catalyst of oxidative desulfurization process. *J. Ind. Eng. Chem.* 39, 66–76. <https://doi.org/10.1016/j.jiec.2016.05.011>.
- Shen, C., Wang, Y.J., Xu, J.H., Luo, G.S., 2016. Oxidative desulfurization of DBT with H₂O₂ catalysed by TiO₂/porous glass. *Green Chem.* 18 (3), 771–781. <https://doi.org/10.1039/c5gc01653c>.
- Trakarnpruk, W., Rujiraworawut, K., 2009. Oxidative desulfurization of Gas oil by polyoxometalates catalysts. *Fuel Process. Technol.* 90 (3), 411–414. <https://doi.org/10.1016/j.fuproc.2008.11.002>.
- Yetilmesoy, K., Demirel, S., Vanderbei, R.J., 2009. Response surface modeling of Pb(II) removal from aqueous solution by *Pistacia vera* L.: box-Behnken experimental design. *J. Hazard. Mater.* 171 (1–3), 551–562. <https://doi.org/10.1016/j.jhazmat.2009.06.035>.
- Zhang, W., Zhang, H., Xiao, J., Zhao, Z., Yu, M., Li, Z., 2014. Carbon nanotube catalysts for oxidative desulfurization of a model diesel fuel using molecular oxygen. *Green Chem.* 16 (1), 211–220. <https://doi.org/10.1039/c3gc41106k>.
- Zhu, W., Xu, Y., Li, H., Dai, B., Xu, H., Wang, C., Chao, Y., Liu, H., 2014. Photocatalytic oxidative desulfurization of dibenzothiophene catalyzed by amorphous TiO₂ in ionic liquid. *Korean J. Chem. Eng.* 31 (2), 211–217. <https://doi.org/10.1007/s11814-013-0224-3>.